

Testing cosmological principle under Copernican principle

Xin Wang^a and Zhiqi Huang^{a,b,1}

^aSchool of Physics and Astronomy, Sun Yat-sen University,
Zhuhai, 519082, P.R.China

^bCSST Science Center for the Guangdong-Hongkong-Macau Greater Bay Area, Sun Yat-sen
University,
Zhuhai, 519082, P.R.China

E-mail: huangzhq25@mail.sysu.edu.cn, wangx898@mail2.sysu.edu.cn

Abstract. Recent observational analyses have revealed potential evidence for a preferred spatial direction in cosmological data. Such directional parameterization inherently places observers at a privileged spatial position, thereby conflicting with the Copernican principle and suffering from the look-elsewhere effect. To restore the Copernican principle which is the foundation of modern astronomy, we propose a stochastic framework for cosmological principle violations. The almost uniform temperature of cosmic microwave background suggests that the deviation of isotropy is negligible ($\lesssim 10^{-5}$ level) on the last scattering surface, which can be used as a zero boundary condition to construct an orthogonal basis below the redshift of recombination. The relative deviation from Hubble diagram of isotropic (Λ CDM or w_0w_a CDM) models is expanded with the orthogonal basis with a hierarchy of increasing resolution. Using this new approach, we test cosmological principle with type Ia supernovae, strong lens time delay, and gravitational-wave standard siren. The data sets are consistent with statistical isotropy on large scales.

ArXiv ePrint: [xxxx.xxxx](https://arxiv.org/abs/xxxx.xxxx)

¹The corresponding author.

Contents

| | | |
|----------|-----------------------------------|----------|
| 1 | Introduction | 1 |
| 2 | Method | 2 |
| 3 | Results | 5 |
| 4 | Discussion and conclusions | 6 |

1 Introduction

The development of modern cosmology is largely based on the cosmological principle, which states that the universe is homogeneous and isotropic on large scales [1]. As an extension of the Copernican principle on cosmological scales, the cosmological principle was initially based more on philosophical considerations than rigorous observational evidence. The evolution of modern cosmology has led to a quantitative refinement of the cosmological principle. According to predictions of the standard cosmological model, the cosmological principle holds approximately valid on scales above 100 Mpc. This characteristic scale arises from the growth of primordial perturbations through gravitational instability, which involves a few more assumptions beyond the Copernican principle. Observational verification of the cosmological principle on scales $\gtrsim 100$ Mpc constitutes a fundamental validation of the cornerstone of the modern standard cosmological model, carrying profound implications for our understanding of cosmic structure formation.

While the earliest empirical evidence for cosmological principle was crude and qualitative, advances in observational cosmology in the last few decades have enabled more rigorous interrogation of the cosmological principle through Bayesian model comparison frameworks. Hints of violation of cosmological principle have been found in multi-probe observations [2–26]. In particular, the bulk flow velocity in a volume of radii ~ 250 Mpc estimated from the CosmicFlows-4 galaxy catalog significantly exceeds the expectation of standard Lambda cold dark matter (Λ CDM) model [5]. A similar dipole asymmetry has been found in the Hubble diagram of the type Ia supernovae (SNe) below redshift ~ 0.1 , although the preferred direction is $\sim 30^\circ$ away from that of the bulk flow velocity [22, 24].

When investigating high-redshift ($z \sim 1$) regimes of the cosmos, where bulk flow measurements become increasingly observationally prohibitive, SNe serve as critical diagnostic tools for probing the cosmological principle on larger scales. Nevertheless, whether high-redshift SNe exhibit statistical isotropy remains contentious, with conflicting conclusions across studies and no definitive consensus to date [19, 23, 27–29]. The most pronounced anisotropy has been found with a hemisphere comparison method, where the discrepancy between cosmological parameters fitted in two hemispheres is maximized by varying the direction of hemisphere splitting [30]. However, even within the hemisphere comparison framework, the statistical significance of cosmological principle violation remains critically sensitive to the choice of parameters and no consensus has been reached. For example, by fitting the Hubble constant H_0 in hemispheres, Ref. [23] finds a preferred direction at 4.39σ significance level, while hemisphere comparison of the deceleration parameter q_0 only yields an 1.78σ significance which can be well interpreted as a statistical fluctuation.

Despite its widespread application, the hemisphere comparison method may introduce three potential problems. First, it places the observer in a privileged position, thereby violating the Copernican principle a priori. Second, the two-dimensional (directional) modeling of cosmic anisotropy on Gpc scales may contradict the observed almost uniform temperature of the cosmic microwave background (CMB). Third, parameters chosen for hemisphere comparison, such as the Hubble constant used in Ref. [23], may be only sensitive to the local data, while their interpretation risks being erroneously generalized to imply global hemispheric asymmetry.

To address these limitations, we propose a new approach that reconciles the Copernican principle by incorporating a full three-dimensional expansion of the Hubble residuals. The CMB last scattering surface serves as a natural boundary where Hubble residuals are known to be negligible ($\lesssim 10^{-5}$). We decompose the Hubble residuals into orthonormal basis functions constructed with zero boundary condition on the last scattering surface, thereby ensuring consistency with CMB isotropy constraints. Finally, the radial dependence of the basis functions separates the contributions from data at different redshifts, thereby avoiding misinterpreting a local anisotropy as a global one.

This paper is organized as follows. Section 2 gives the detailed description of our method and the data sets that we use. Results are given in Section 3. Section 4 discusses and concludes. Throughout the paper we use natural units. The scale factor a is normalized to unity at redshift zero. The matter abundance parameter Ω_m is defined as the ratio between the current background matter density and the critical density $\frac{3H_0^2}{8\pi G}$, where G is the Newton's gravitational constant. The right ascension (RA) and declination (DEC) are defined in the International Celestial Reference System (ICRS), while spherical harmonics are evaluated in the Galactic coordinate frame.

2 Method

A point-like object at redshift z and in direction \mathbf{n} is labeled with a reference coordinate $(\tilde{r}(z), \mathbf{n})$, where $\tilde{r}(z)$ is the comoving distance in a reference isotropic model, such as Λ CDM. The true comoving distance of the object, which we allow to be anisotropic, is decomposed into orthonormal functions in the reference coordinate space,

$$r(z, \mathbf{n}) = \tilde{r}(z) \left[1 + \sum_{i=1}^{\infty} \sum_{\ell=0}^{\infty} \sum_{m=-\ell}^{\ell} C_{i\ell m} j_{\ell} \left(\frac{\mu_{\ell i} \tilde{r}(z)}{\tilde{r}(z_{\text{rec}})} \right) Y_{\ell m}(\mathbf{n}) \right], \quad (2.1)$$

where $Y_{\ell m}$ is the spherical harmonic function, and $\mu_{\ell i}$ is the i -th positive root of the spherical Bessel function j_{ℓ} . The recombination redshift $z_{\text{rec}} \approx 1089$ has been accurately measured by CMB experiments in a very model-insensitive way [31], and is therefore fixed in our calculation. By construction, $r(z_{\text{rec}}, \mathbf{n})$ is identical to $\tilde{r}(z_{\text{rec}})$ in all directions, thereby satisfying the CMB isotropy constraint.

In practice, with only $\sim 10^3$ currently available data points, we may only constrain the model to a quite limited spatial resolution, represented by a truncated radial index i_{max} and a truncated angular index ℓ_{max} . Moreover, for programming convenience we replace the complex spherical harmonics with real ones, defined as

$$\mathcal{Y}_{\ell m} \equiv \begin{cases} \frac{Y_{\ell m} + (-1)^m Y_{\ell, -m}}{\sqrt{2}}, & m > 0; \\ Y_{\ell m}, & m = 0; \\ \frac{Y_{\ell, -m} - (-1)^m Y_{\ell m}}{\sqrt{2}i}, & m < 0. \end{cases} \quad (2.2)$$

Finally, we will drop the $\ell = 0$ component which can be absorbed into the reference isotropic model. The actual model used for parameter inference is then

$$r(z, \mathbf{n}) = \tilde{r}(z) \left[1 + \sum_{i=1}^{i_{\max}} \sum_{\ell=1}^{\ell_{\max}} \sum_{m=-\ell}^{\ell} C_{i\ell m} \mathbf{j}_{\ell} \left(\frac{\mu_{\ell i} \tilde{r}(z)}{\tilde{r}(z_{\text{rec}})} \right) \mathcal{Y}_{\ell m}(\mathbf{n}) \right]. \quad (2.3)$$

We consider three reference isotropic models: Λ CDM, $w_0 w_a$ CDM, and PAge. Here $w_0 w_a$ CDM refers to the dynamic dark energy model where dark energy equation of state is parameterized as $w(a) = w_0 + w_a(1 - a)$ [32, 33]; PAge refers to the Parameterization based cosmic Age, which is designed for more generic considerations in opposition to the specific scenario of two dark fluids (dark matter + dark energy) [34–38]. Compared to Λ CDM, PAge does not parameterize the dark components, but contains two new parameters: p_{age} that is the age of the universe in unit of H_0^{-1} and η that quantifies the deviation from Einstein de Sitter cosmology. Because we have included the SH0ES distance-ladder data, the parameter set also contains M , the absolute magnitude of SNe. The cosmological parameters are sampled with the following uniform priors: $\Omega_m \in [0.2, 0.4]$, $H_0 \in [60, 90] \text{ km} \cdot \text{s}^{-1} \text{Mpc}^{-1}$, $w_0 \in [-3, 1]$, $w_a \in [-3, 2]$, $p_{\text{age}} \in [0.8, 1.5]$, $\eta \in [-1, 1]$, and $M \in [-25, -15]$. The anisotropy coefficients are sampled with a uniform prior $C_{i\ell m} \in [-5, 5]$, $\forall i, \ell, m$. We also apply priors $13 \text{ Gpc} < \tilde{r}(z_{\text{rec}}) < 15 \text{ Gpc}$ and $w_0 + w_a < 0$ to ensure that the models do not run into nonphysical parameter space.

The primary data sets we use for this study are the Pantheon+ and SH0ES supernovae [39], publicly available at <https://github.com/PantheonPlusSH0ES/DataRelease>. To avoid large redshift contribution from peculiar velocity, we only use a subset of 1657 SNe with CMB-frame redshift $z > 0.01$. We modify the publicly available likelihood to incorporate the revised anisotropic comoving distance, Eq. (2.3). Hereafter for brevity we will implicitly refer the selected 1657 SNe as “Pantheon+”, without specifying the inclusion of SH0ES and the exclusion of the $z < 0.01$ subset.

To check consistency between Pantheon+ and other cosmological data sets, we optionally include additional multi-probe data that are collectively shown in Figure 1. The extra data include seven data points of strong lens time delay (SLTD) [40, 41], one data point of gravitational-wave standard siren (GWSS) [42], and 1635 SNe from the full five year of the Dark Energy Survey (DES5YR) SN program [43]. The summary statistics of SLTD are listed in Table 1. The GWSS data is a constraint on the angular diameter distance $d_A(z = 0.01006, \text{RA} = 197.4487^\circ, \text{DEC} = -23.3840^\circ) = 43.8_{-6.9}^{+2.9} \text{ Mpc}$, where $d_A(z, \mathbf{n}) = \frac{r(z, \mathbf{n})}{1+z}$. The DES5YR SN data and likelihood are publicly available at <https://github.com/des-science/DES-SN5YR>. We also modified the DES5YR SN likelihood to exclude the 194 low- z SNe that largely overlap with Pantheon+ and to incorporate the anisotropic model described by Eq. (2.3).

We run Markov Chain Monte Carlo (MCMC) simulations to infer cosmological parameters as well as the anisotropy coefficients $C_{i\ell m}$ ’s. A detection of nonzero $C_{i\ell m}$ typically implies a violation of cosmological principle, though in the high-resolution (large ℓ_{\max} , i_{\max}) case more careful Bayesian model comparison should be done to avoid the over-fitting problem. A more convenient approach is to use the Gaussian approximation to estimate the statistical significance of the preference for anisotropy. When the posterior of parameters are obtained from Markov Chains, we compute the mean and the covariance matrix of the $C_{i\ell m}$ coefficients, denoted as v and Cov respectively. The tail probability of the isotropic model

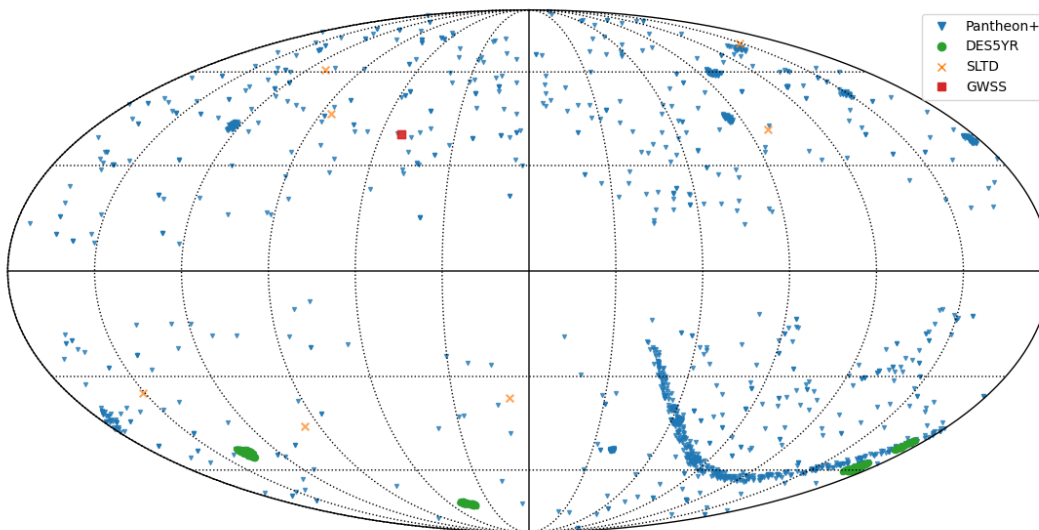


Figure 1. Galactic coordinates of the data.

Table 1. Summary statistics of the strong lens time delay data.

| Lens name | RA(deg) | DEC(deg) | z_l | z_s | $\frac{r(z_l)r(z_s)}{r(z_s)-r(z_l)}$ (Mpc) |
|-----------------------|-----------|-----------|--------|-------|--|
| B1608+656[44, 45] | 242.3081 | 65.5411 | 0.6304 | 1.394 | 5156^{+296}_{-236} |
| RXJ1131-1231[46, 47] | 172.9644 | -12.5329 | 0.295 | 0.654 | 2096^{+98}_{-83} |
| HE0435-1223[47, 48] | 69.5619 | -12.28745 | 0.4546 | 1.693 | 2707^{+183}_{-168} |
| SDSSJ1206+4332[49] | 181.62361 | 43.53856 | 0.745 | 1.789 | 5769^{+589}_{-471} |
| WFI2033-4723[50] | 308.4257 | -47.3956 | 0.6575 | 1.662 | 4784^{+399}_{-248} |
| PG1115+080[47] | 169.57035 | 7.76627 | 0.311 | 1.722 | 1470^{+137}_{-127} |
| DESJ0408-5354[41, 51] | 62.0905 | -53.8999 | 0.597 | 2.375 | 3382^{+146}_{-115} |

(all $C_{\ell m} = 0$) in the Gaussian approximation is given by

$$p = \frac{2^{1-\frac{N_c}{2}}}{\Gamma\left(\frac{N_c}{2}\right)} \int_{\rho_0}^{\infty} e^{-\rho^2/2} \rho^{N_c-1} d\rho, \quad (2.4)$$

where $N_c = i_{\max}\ell_{\max}(\ell_{\max} + 2)$ is the total number of the $C_{\ell m}$ coefficients and $\rho_0 \equiv \sqrt{v^T \text{Cov}^{-1} v}$. The preference for anisotropy can also be framed in more intuitive terms by expressing its significance in sigma units. The number of sigmas, $n_{\sigma}^{\text{aniso}}$, is linked to the tail probability via $p = \text{erfc}\left(\frac{n_{\sigma}^{\text{aniso}}}{\sqrt{2}}\right)$, where erfc is the complementary error function.

We also employ the Akaike Information Criterion (AIC) as a measure that is complementary to the Bayesian analysis with Gaussian approximation. Specifically, AIC is defined as:

$$\text{AIC} = \chi_{\min}^2 + 2k, \quad (2.5)$$

where χ^2_{\min} is the minimum chi-square statistic and k is the number of free parameters. Lower AIC values indicate models that better balance fit and complexity, with the penalty term $2k$ discouraging unnecessary parameterization.

3 Results

Table 2 summarizes the analyses of the Pantheon+ SNe with various reference isotropic models and anisotropy resolutions. At $\lesssim 1.5\sigma$ confidence level, the data allow all the anisotropy coefficients C_{ilm} 's to be zero simultaneously. The isotropic models whose AICs are significantly lower are favored by the data. Thus, up to the resolution we have tested, Pantheon+ is in excellent agreement with cosmological principle.

Among the isotropic models, PAge has the lowest AIC. However, no strong preference for either of the isotropic models should be claimed, as the differences between the AICs of the isotropic models are small ($\lesssim 2$).

Table 2. Statistical significance of anisotropy in Pantheon+ SNe

| reference model | ℓ_{\max} | i_{\max} | $n_{\sigma}^{\text{aniso}}$ | χ^2_{\min} | AIC |
|-----------------|---------------|------------|-----------------------------|-----------------|--------|
| Λ CDM | 0 | 0 | - | 1455.1 | 1461.1 |
| | 1 | 1 | 0.87 | 1452.6 | 1464.6 |
| | 1 | 2 | 0.70 | 1450.2 | 1468.2 |
| | 1 | 3 | 0.39 | 1449.5 | 1473.5 |
| | 1 | 4 | 0.35 | 1448.9 | 1478.9 |
| | 2 | 1 | 0.62 | 1449.5 | 1471.5 |
| | 2 | 2 | 1.15 | 1437.2 | 1475.2 |
| | 3 | 1 | 1.29 | 1435.9 | 1471.9 |
| w_0w_a CDM | 0 | 0 | - | 1451.7 | 1461.7 |
| | 1 | 1 | 0.34 | 1450.3 | 1466.3 |
| PAge | 0 | 0 | - | 1451.7 | 1459.7 |
| | 1 | 1 | 0.39 | 1450.4 | 1464.4 |

Next, we include DES5YR SNe, SLTD and GWSS into our analyses. It is not a common practice to merge supernova data sets with different calibration and modeling. Specifically, DES5YR uses the SALT3 light-curve fitting model [52] as opposed to the SALT2 [53] that is used in Pantheon+. The major difference between the two data sets is modeled with $\Delta\mathcal{M} = \mathcal{M}_{\text{DES5YR}} - \mathcal{M}_{\text{Pantheon+}}$, the difference between the standardized SN absolute magnitudes of the two data sets. By comparing the common samples in Pantheon+ and DES5YR, Ref. [54] found a significant offset between $\Delta\mathcal{M}$ at $z < 0.1$ and that at higher redshift. According to Ref. [55], the origin of this offset is mainly due to the upgrade of intrinsic scatter model from SALT2 to SALT3 and improvements to the host stellar mass estimates of some low- z samples. Nevertheless, we have removed the $z < 0.1$ samples from DES5YR to avoid a big impact from the known $\Delta\mathcal{M}$ offset. At $z > 0.1$, there are still a few percent of DES5YR samples overlapping with Pantheon+. We do not remove them from either catalog, as they help to diagnose whether a constant \mathcal{M} at $z > 0.1$ is a good model. We have checked

that double counting them in the likelihood leads to very minor impact on cosmological parameters.

Table 3. Testing anisotropy with SNe (Pantheon+&DES5YR) + SLTD + GWSS

| reference model | ℓ_{\max} | i_{\max} | $n_{\sigma}^{\text{aniso}}$ | χ_{\min}^2 | AIC | posterior of $\Delta\mathcal{M}$ |
|---------------------|---------------|------------|-----------------------------|-----------------|--------|----------------------------------|
| ΛCDM | 0 | 0 | - | 2911.8 | 2919.8 | 0.0196 ± 0.0067 |
| | 1 | 1 | 1.04 | 2909.1 | 2923.1 | 0.0290 ± 0.0085 |
| | 1 | 2 | 1.10 | 2906.3 | 2926.3 | 0.0294 ± 0.0083 |
| | 2 | 1 | 1.22 | 2903.5 | 2927.5 | 0.0291 ± 0.0085 |
| $w_0w_a\text{CDM}$ | 0 | 0 | - | 2908.8 | 2920.8 | 0.0309 ± 0.0079 |
| | 1 | 1 | 0.44 | 2907.6 | 2925.6 | 0.0357 ± 0.0088 |
| | 2 | 1 | 1.37 | 2900.5 | 2928.5 | 0.0362 ± 0.0094 |
| PAGe | 0 | 0 | - | 2908.8 | 2918.8 | 0.0318 ± 0.0086 |
| | 1 | 1 | 0.73 | 2907.7 | 2923.7 | 0.0350 ± 0.0091 |
| | 2 | 1 | 0.86 | 2902.0 | 2928.0 | 0.0351 ± 0.0095 |

Table 3 summarizes the results of model comparison, which again favor the isotropic models. Figure 2 shows the marginalized posteriors of the anisotropy coefficients of the $\ell_{\max} = 2$, $i_{\max} = 1$ case as a typical example. In all cases, the cosmological principle ($C_{ilm} = 0, \forall i, \ell, m$) is in excellent agreement with the joint multi-probe data.

As the last column of Table 3 shows, a nonzero $\Delta\mathcal{M}$ is found at $\gtrsim 3\sigma$ confidence level in all cases. The posterior of $\Delta\mathcal{M}$ has a noticeable cosmology dependence. In particular, the mean value of $\Delta\mathcal{M}$ shifts by about 1.5σ from isotropic ΛCDM to models beyond ΛCDM (anisotropic or $w_0w_a\text{CDM}$ or PAGe). The degeneracy between $\Delta\mathcal{M}$ and cosmology indicates that there is still a trend of redshift evolution of $\Delta\mathcal{M}$ at $z > 0.1$.

As more data accumulates, cosmological information does not seem converge towards ΛCDM . Both the isotropic $w_0w_a\text{CDM}$ and the isotropic PAGe remain competitive in terms of low AICs. Moreover, the inferred cosmological parameters, some of which are shown in Figure 3, are not fully consistent with their values constrained by CMB+ ΛCDM . For isotropic ΛCDM model we obtain $H_0 = 72.8 \pm 0.75 \text{ km/s/Mpc}$, in 5.9σ tension with the Planck value $67.4 \pm 0.5 \text{ km/s/Mpc}$ [31]. Compared to the SH0ES result $H_0 = 73.04 \pm 1.04 \text{ km/s/Mpc}$, our tighter constraint on H_0 is mainly due to inclusion of the SLTD data which also measures H_0 . For isotropic w_0w_a model we find $w_0 = -0.89 \pm 0.07$ and $w_a = 0.25 \pm 0.45$, i.e., no evidence for the recently claimed dynamic dark energy [56–58]. However, due to the controversial joint usage of different SN catalogs and the hint of redshift evolution of $\Delta\mathcal{M}$, these cosmological results based on the constant $\Delta\mathcal{M}$ model should be quoted with caution.

4 Discussion and conclusions

In this work, we apply a full 3D expansion of anisotropic modes to test cosmological principle without assuming a privileged position of the observers, thereby effectively taking into account the look-elsewhere effect. Applying the new method to the Pantheon+ supernova catalog, and to Pantheon+ combined with DES5YR SNe, SLTD, and GWSS, we find no

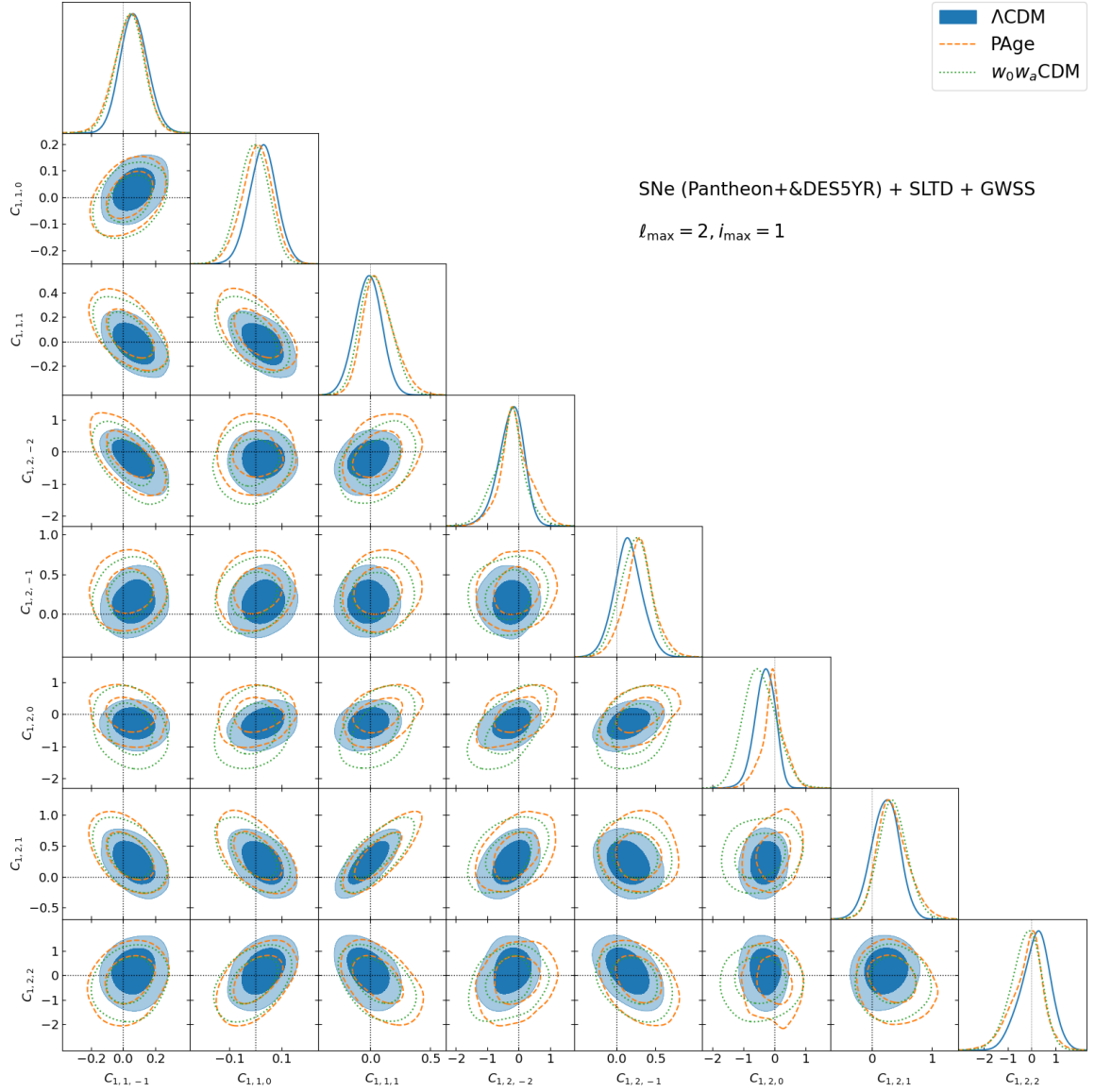


Figure 2. Marginalized 68.3% and 95.4% confidence-level constraints on anisotropy coefficients.

hint of anisotropy. These results deny the global hemisphere asymmetry found in Ref. [23]. As we have emphasized in the introduction, a seemingly global asymmetry found with the hemisphere comparison method could be actually local, as the chosen parameter (H_0) may only be sensitive to the local (distance-ladder) data. Therefore, the hemisphere asymmetry identified in Ref. [23] may be another manifestation of the local dipole-like anisotropy at $z \lesssim 0.1$ [5, 22, 24].

Due to the limited size of data, we can only expand the Hubble residuals to low resolutions with $i_{\max}, \ell_{\max} \sim$ a few. Therefore, only anisotropies on large (\sim Gpc) scales have been tested, and the local $z \lesssim 0.1$ anisotropy found by Ref. [22] is missed in this work. To test the cosmological principle in our local neighborhood, a different expansion basis should be

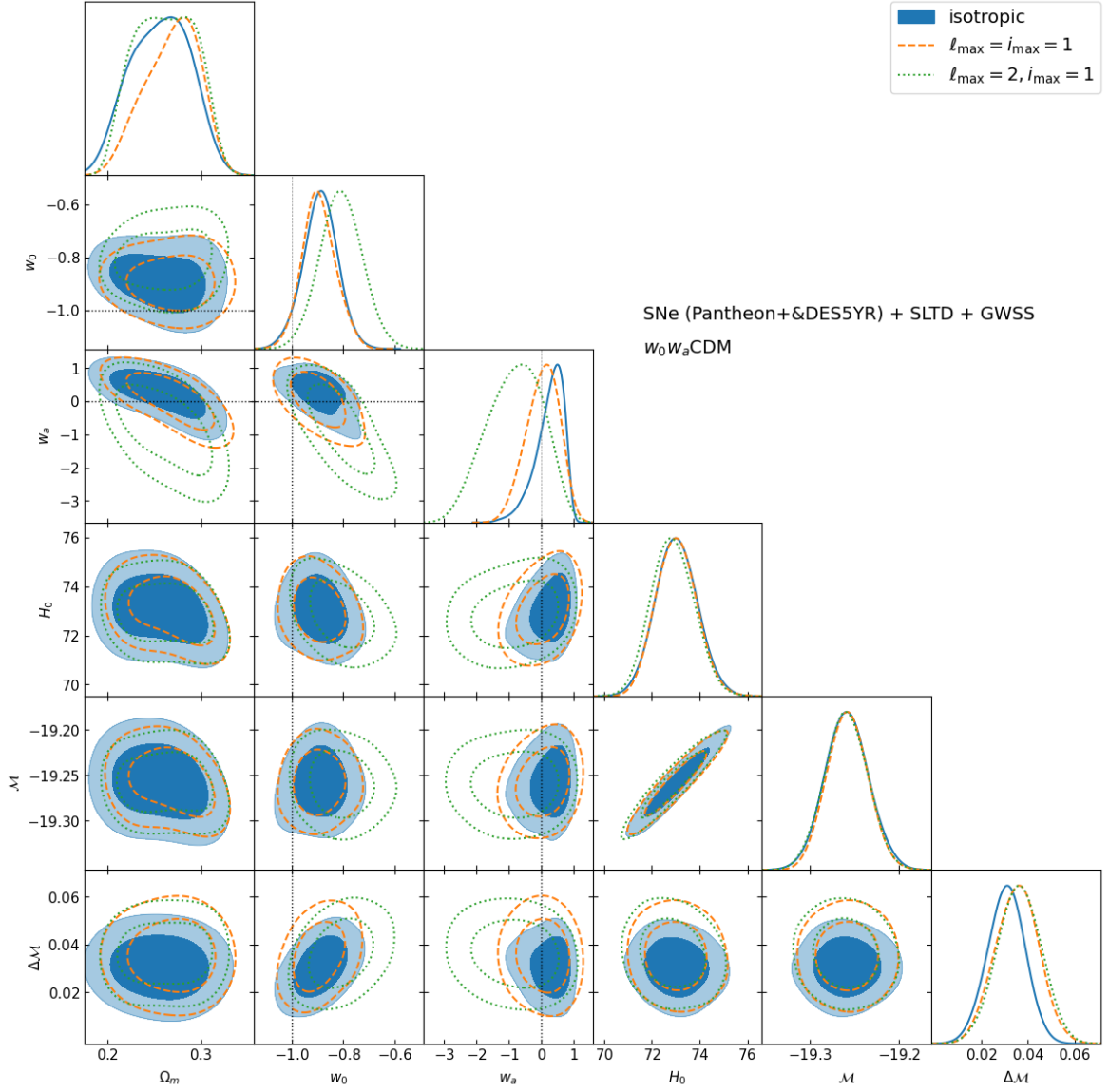


Figure 3. Marginalized 68.3% and 95.4% confidence-level constraints on cosmological parameters.

used. These extended analyses will be presented in a companion paper [59], where we focus on the local dipole asymmetry and its impact on the Hubble tension and the preference for dynamic dark energy.

Acknowledgments

This work is supported by the National SKA Program of China (grant No. 2020SKA0110402), the National Natural Science Foundation of China (NSFC, grant No. 12073088), and the National Key R&D Program of China (grant No. 2020YFC2201600).

References

- [1] P.K. Aluri et al., *Is the observable Universe consistent with the cosmological principle?*, *Class. Quant. Grav.* **40** (2023) 094001 [[2207.05765](#)].
- [2] R. Watkins, H.A. Feldman and M.J. Hudson, *Consistently Large Cosmic Flows on Scales of 100 Mpc/h: a Challenge for the Standard LCDM Cosmology*, *Mon. Not. Roy. Astron. Soc.* **392** (2009) 743 [[0809.4041](#)].
- [3] H.A. Feldman, R. Watkins and M.J. Hudson, *Cosmic Flows on 100 Mpc/h Scales: Standardized Minimum Variance Bulk Flow, Shear and Octupole Moments*, *Mon. Not. Roy. Astron. Soc.* **407** (2010) 2328 [[0911.5516](#)].
- [4] K. Migkas, F. Pacaud, G. Schellenberger et al., *Cosmological implications of the anisotropy of ten galaxy cluster scaling relations*, *Astronomy & Astrophysics* **649** (2021) A151 [[2103.13904](#)].
- [5] R. Watkins, T. Allen, C.J. Bradford, A. Ramon, A. Walker, H.A. Feldman et al., *Analysing the large-scale bulk flow using cosmicflows4: increasing tension with the standard cosmological model*, *Mon. Not. Roy. Astron. Soc.* **524** (2023) 1885 [[2302.02028](#)].
- [6] M. Tegmark, A. de Oliveira-Costa and A. Hamilton, *A high resolution foreground cleaned CMB map from WMAP*, *Phys. Rev. D* **68** (2003) 123523 [[astro-ph/0302496](#)].
- [7] R.C. Helling, P. Schupp and T. Tesileanu, *CMB statistical anisotropy, multipole vectors and the influence of the dipole*, *Phys. Rev. D* **74** (2006) 063004 [[astro-ph/0603594](#)].
- [8] L.R. Abramo, A. Bernui, I.S. Ferreira, T. Villela and C.A. Wuensche, *Alignment Tests for low CMB multipoles*, *Phys. Rev. D* **74** (2006) 063506 [[astro-ph/0604346](#)].
- [9] A. Gruppuso and K.M. Gorski, *Large scale directional anomalies in the WMAP 5yr ILC map*, *JCAP* **03** (2010) 019 [[1002.3928](#)].
- [10] L. Polastri, *Cosmic Microwave Background large-scale directional anomalies as seen by Planck and WMAP*, *J. Phys. Conf. Ser.* **841** (2017) 012008.
- [11] PLANCK collaboration, *Planck 2018 results. VII. Isotropy and Statistics of the CMB*, *Astron. Astrophys.* **641** (2020) A7 [[1906.02552](#)].
- [12] D. Hutsemekers and H. Lamy, *Confirmation of the existence of coherent orientations of quasar polarization vectors on cosmological scales*, *Astron. Astrophys.* **367** (2001) 381 [[astro-ph/0012182](#)].
- [13] P. Jain, G. Narain and S. Sarala, *Large scale alignment of optical polarizations from distant QSOs using coordinate invariant statistics*, *Mon. Not. Roy. Astron. Soc.* **347** (2004) 394 [[astro-ph/0301530](#)].
- [14] R. Shurtleff, *A Large Scale Pattern from Optical Quasar Polarization Vectors*, [1311.6118](#).
- [15] V. Pelgrims and D. Hutsemekers, *Polarization alignments of quasars from the JVAS/CLASS 8.4-GHz surveys*, *Mon. Not. Roy. Astron. Soc.* **450** (2015) 4161 [[1503.03482](#)].
- [16] I. Antoniou and L. Perivolaropoulos, *Searching for a cosmological preferred axis: Union2 data analysis and comparison with other probes*, *Journal of Cosmology and Astroparticle Physics* **2010** (2010) 012–012.
- [17] R.-G. Cai and Z.-L. Tuo, *Direction Dependence of the Deceleration Parameter*, *JCAP* **02** (2012) 004 [[1109.0941](#)].
- [18] X. Yang, F.Y. Wang and Z. Chu, *Searching for a preferred direction with Union2.1 data*, *Mon. Not. Roy. Astron. Soc.* **437** (2014) 1840 [[1310.5211](#)].
- [19] D. Zhao, Y. Zhou and Z. Chang, *Anisotropy of the Universe via the Pantheon supernovae sample revisited*, *Mon. Not. Roy. Astron. Soc.* **486** (2019) 5679 [[1903.12401](#)].

- [20] J.P. Hu, Y.Y. Wang and F.Y. Wang, *Testing cosmic anisotropy with Pantheon sample and quasars at high redshifts*, *Astron. Astrophys.* **643** (2020) A93 [[2008.12439](#)].
- [21] R. Mc Conville and E. Ó Colgáin, *Anisotropic distance ladder in Pantheon+supernovae*, *Physical Review D* **108** (2023) 123533 [[2304.02718](#)].
- [22] L. Tang, H.-N. Lin, L. Liu and X. Li, *Consistency of Pantheon+ supernovae with a large-scale isotropic universe*, *Chinese Physics C* **47** (2023) 125101 [[2309.11320](#)].
- [23] J. Hu, J. Hu, X. Jia, B. Gao and F. Wang, *Testing cosmic anisotropy with Padé approximations and the latest Pantheon+ sample*, *Astron. Astrophys.* **689** (2024) A215 [[2406.14827](#)].
- [24] A. Sah, M. Rameez, S. Sarkar and C. Tsagas, *Anisotropy in Pantheon+ supernovae*, *arXiv e-prints* (2024) [arXiv:2411.10838](#) [[2411.10838](#)].
- [25] A. Antony, S. Appleby, W.L. Matthewson and A. Shafieloo, *Isotropy Test with Quasars Using Method of Smoothed Residuals*, *arXiv e-prints* (2025) [arXiv:2505.07439](#) [[2505.07439](#)].
- [26] A.M. Lopez, R. Clowes and G. Williger, *Investigating ultra-large large-scale structures: potential implications for cosmology*, *Philosophical Transactions of the Royal Society of London Series A* **383** (2025) 20240029 [[2409.14894](#)].
- [27] H.-K. Deng and H. Wei, *Null signal for the cosmic anisotropy in the Pantheon supernovae data*, *Eur. Phys. J. C* **78** (2018) 755 [[1806.02773](#)].
- [28] J.P. Hu, Y.Y. Wang, J. Hu and F.Y. Wang, *Testing the cosmological principle with the Pantheon+ sample and the region-fitting method*, *Astronomy & Astrophysics* **681** (2024) A88 [[2310.11727](#)].
- [29] Z.-F. Yang, D.-W. Yao, M. Le Delliou and K. Wang, *Model-independent test of the cosmic anisotropy with inverse distance ladder*, *European Physical Journal C* **85** (2025) 339 [[2407.19278](#)].
- [30] D.J. Schwarz and B. Weinhorst, *(An)isotropy of the Hubble diagram: comparing hemispheres*, *Astronomy & Astrophysics* **474** (2007) 717 [[0706.0165](#)].
- [31] Planck Collaboration, N. Aghanim, Y. Akrami, M. Ashdown et al., *Planck 2018 results. VI. Cosmological parameters*, *Astronomy & Astrophysics* **641** (2020) A6 [[1807.06209](#)].
- [32] M. Chevallier and D. Polarski, *Accelerating universes with scaling dark matter*, *Int. J. Mod. Phys. D* **10** (2001) 213 [[gr-qc/0009008](#)].
- [33] E.V. Linder, *Exploring the expansion history of the universe*, *Phys. Rev. Lett.* **90** (2003) 091301 [[astro-ph/0208512](#)].
- [34] Z. Huang, *Supernova Magnitude Evolution and PAge Approximation*, *Astrophysical Journal Letters* **892** (2020) L28 [[2001.06926](#)].
- [35] L. Huang, Z.-Q. Huang, Z.-Y. Li and H. Zhou, *A more accurate Parameterization based on cosmic Age (MAPAge)*, *Research in Astronomy and Astrophysics* **21** (2021) 277 [[2108.03959](#)].
- [36] Z. Huang, *Thawing k-essence dark energy in the PAge space*, *Communications in Theoretical Physics* **74** (2022) 095404 [[2204.09713](#)].
- [37] J. Wang, Z. Huang, Y. Yao, J. Liu, L. Huang and Y. Su, *A PAge-like Unified Dark Fluid model*, *JCAP* **2024** (2024) 053 [[2405.05798](#)].
- [38] Y. Su, Z. Huang, J. Wang, Y. Yao and J. Liu, *The dark side of the universe may be more harmonic than we thought*, *arXiv e-prints* (2025) [arXiv:2504.00536](#) [[2504.00536](#)].
- [39] D. Brout, D. Scolnic, B. Popovic, A.G. Riess et al., *The Pantheon+ Analysis: Cosmological Constraints*, *Astrophysical Journal* **938** (2022) 110 [[2202.04077](#)].

- [40] K.C. Wong, S.H. Suyu, G.C.F. Chen, C.E. Rusu, M. Millon, D. Sluse et al., *H0LiCOW - XIII. A 2.4 per cent measurement of H_0 from lensed quasars: 5.3 σ tension between early- and late-Universe probes*, *MNRAS* **498** (2020) 1420 [[1907.04869](#)].
- [41] A.J. Shajib, S. Birrer, T. Treu, A. Agnello, E.J. Buckley-Geer, J.H.H. Chan et al., *STRIDES: a 3.9 per cent measurement of the Hubble constant from the strong lens system DES J0408-5354*, *MNRAS* **494** (2020) 6072 [[1910.06306](#)].
- [42] B.P. Abbott, R. Abbott, T.D. Abbott, F. Acernese et al., *A gravitational-wave standard siren measurement of the Hubble constant*, *Nature* **551** (2017) 85 [[1710.05835](#)].
- [43] DES Collaboration, T.M.C. Abbott, M. Acevedo, M. Agüena, A. Alarcon et al., *The Dark Energy Survey: Cosmology Results with ~ 1500 New High-redshift Type Ia Supernovae Using the Full 5 yr Data Set*, *Astrophysical Journal Letters* **973** (2024) L14 [[2401.02929](#)].
- [44] S.H. Suyu, P.J. Marshall, M.W. Auger, S. Hilbert, R.D. Blandford, L.V.E. Koopmans et al., *Dissecting the Gravitational Lens B1608+656. II. Precision Measurements of the Hubble Constant, Spatial Curvature, and the Dark Energy Equation of State*, *Astrophys. J.* **711** (2010) 201 [[0910.2773](#)].
- [45] I. Jee, S. Suyu, E. Komatsu, C.D. Fassnacht, S. Hilbert and L.V.E. Koopmans, *A measurement of the Hubble constant from angular diameter distances to two gravitational lenses*, [1909.06712](#).
- [46] S.H. Suyu et al., *Cosmology from gravitational lens time delays and Planck data*, *Astrophys. J. Lett.* **788** (2014) L35 [[1306.4732](#)].
- [47] H0LiCOW collaboration, *A SHARP view of H0LiCOW: H_0 from three time-delay gravitational lens systems with adaptive optics imaging*, *Mon. Not. Roy. Astron. Soc.* **490** (2019) 1743 [[1907.02533](#)].
- [48] H0LiCOW collaboration, *H0LiCOW – IV. Lens mass model of HE 0435–1223 and blind measurement of its time-delay distance for cosmology*, *Mon. Not. Roy. Astron. Soc.* **465** (2017) 4895 [[1607.01403](#)].
- [49] H0LiCOW collaboration, *H0LiCOW - IX. Cosmographic analysis of the doubly imaged quasar SDSS 1206+4332 and a new measurement of the Hubble constant*, *Mon. Not. Roy. Astron. Soc.* **484** (2019) 4726 [[1809.01274](#)].
- [50] H0LiCOW collaboration, *H0LiCOW XII. Lens mass model of WFI2033 – 4723 and blind measurement of its time-delay distance and H_0* , *Mon. Not. Roy. Astron. Soc.* **498** (2020) 1440 [[1905.09338](#)].
- [51] A. Agnello et al., *Models of the strongly lensed quasar DES J0408–5354*, *Mon. Not. Roy. Astron. Soc.* **472** (2017) 4038 [[1702.00406](#)].
- [52] W.D. Kenworthy, D.O. Jones, M. Dai, R. Kessler, D. Scolnic, D. Brout et al., *SALT3: An Improved Type Ia Supernova Model for Measuring Cosmic Distances*, *Astrophysical Journal* **923** (2021) 265 [[2104.07795](#)].
- [53] J. Guy, P. Astier, S. Baumont, D. Hardin, R. Pain, N. Regnault et al., *SALT2: using distant supernovae to improve the use of type Ia supernovae as distance indicators*, *Astronomy & Astrophysics* **466** (2007) 11 [[astro-ph/0701828](#)].
- [54] G. Efstathiou, *Evolving dark energy or supernovae systematics?*, *MNRAS* **538** (2025) 875 [[2408.07175](#)].
- [55] M. Vincenzi, R. Kessler, P. Shah, J. Lee et al., *Comparing the DES-SN5YR and Pantheon+ SN cosmology analyses: Investigation based on “Evolving Dark Energy or Supernovae systematics?”*, *arXiv e-prints* (2025) [arXiv:2501.06664](#) [[2501.06664](#)].
- [56] DESI collaboration, *DESI 2024 VI: cosmological constraints from the measurements of baryon acoustic oscillations*, *JCAP* **02** (2025) 021 [[2404.03002](#)].

- [57] DESI collaboration, *DESI DR2 Results II: Measurements of Baryon Acoustic Oscillations and Cosmological Constraints*, [2503.14738](#).
- [58] T.M.C. Abbott, M. Acevedo, M. Adamow et al., *Dark Energy Survey: implications for cosmological expansion models from the final DES Baryon Acoustic Oscillation and Supernova data*, *arXiv e-prints* (2025) [arXiv:2503.06712](#) [[2503.06712](#)].
- [59] Z. Huang, *The odd local universe, hubble tension and dynamic dark energy, in preparation* (2025) .